

PHYSICS OF SUPERNOVAE*

D. K. NADYOZHIN and V. S. IMSHENNIK

*A. I. Alikhanov Institute for Theoretical and Experimental Physics
B. Chermushkinskaya St. 25, RU-117218, Moscow, Russia*

The origin of cosmic rays (CR) is supposed to be closely connected with supernovae (SNe) which create the conditions favorable for various mechanisms of the CR acceleration to operate effectively. First, modern ideas about the physics of the SN explosion are briefly discussed: the explosive thermonuclear burning in degenerate white dwarfs resulting in Type Ia SNe and the gravitational collapse of stellar cores giving rise to other types of SNe (Ib, Ic, IIL, IIP). Next, we survey some global properties of the SNe of different types: the total explosion energy distribution of various components (kinetic energy of the hydrodynamic flow, electromagnetic radiation, temporal behavior of the neutrino emission and individual energies of different neutrino flavors). Then, we discuss in the possibility of direct hydrodynamic acceleration by the shock wave breakout and the properties of the SN shocks in the circumstellar medium. Then the properties of the neutrino radiation from the core-collapse SNe and a possibility to incorporate both the LSD Mont Blanc neutrino event and that recorded by the K II and IMB detectors into a single scenario are described in detail. Finally, the issues of the neutrino nucleosynthesis and of the connection between supernova and gamma-ray bursts are discussed.

Keywords: supernovae; neutrino; stellar nucleosynthesis.

1. Basic Properties of Supernovae

Physically, there are two fundamental types of supernovae (SNe): the thermonuclear SNe and the core-collapse ones, represented by Type Ia SNe (SN Ia) and by Type II, Ib, and Ic SNe, respectively. The SN Ia show no hydrogen in their spectra and constitute quite a homogeneous sample of objects. The core-collapse SNe are subdivided into several types depending on the amount of hydrogen hanging around the stellar core just before it begins to collapse. Type Ib and Ic SNe have virtually no hydrogen left. The Ic SNe seem to have lost a fair amount of their helium as well.

Type II SNe are represented by the subtypes IIP (plateau shaped light curves, $\sim 10 M_{\odot}$ of hydrogen in their envelopes), IIL (linearly decaying light curves, $\lesssim 1 M_{\odot}$ of hydrogen), and IIn (with some hydrogen in an extended envelope formed by dense stellar wind).

1.1. Thermonuclear supernovae

The SN Ia light curves are powered by the $^{56}\text{Ni} \rightarrow ^{56}\text{Co} \rightarrow ^{56}\text{Fe}$ beta-decay on average of $\approx 0.6 M_{\odot}$ of ^{56}Ni synthesized as a result of explosive carbon-oxygen (CO) burning in a degenerate *Chandrasekhar mass* ($M \approx 1.4 M_{\odot}$) white dwarf. The total energy of the

*Invited lecture at the 19th European Cosmic Ray Symposium, August 30 – September 3, 2004, Florence, Italy

electromagnetic emission is of $\approx 6 \times 10^{49}$ erg, most of this energy being radiated in optical and infrared wavelengths and only a fraction being carried away by X-rays and gamma-photons that managed to escape the scattering off by the expanding envelope. The explosion energy $E_{\text{exp}} \approx 10^{51}$ erg comes from the difference in nuclear binding energies of the initial carbon-oxygen mixture and the final products of thermonuclear burning (mainly ^{56}Ni – the most tightly bounded nucleus among all those consisting of equal numbers of neutrons and protons). Finally, almost all E_{exp} turns out to be converted into the kinetic energy of expanding matter. The white dwarf proves to be totally disrupted by the explosion, no stellar remnant being left. The mean velocity of the expanding debris is estimated to be $\langle u \rangle = \sqrt{2E_{\text{exp}}/M} \approx 8,000$ km/s.

Although observationally and theoretically the above concept is considered to be a well-founded conjecture, there remains a big unsolved problem relating to the mode of thermonuclear CO-burning. The most important issue is an interplay between the deflagration and detonation regimes of burning which is controlled by different instabilities of turbulent thermonuclear flame propagating in degenerate matter and by the behavior of the white dwarf as a whole in response to the onset of the burning (pre-expansion,^{1,2} radial pulsations^{3,4}). Several astrophysical groups are currently engaged in an extensive investigation of the thermonuclear burning in Type Ia supernovae (see Refs. 5, 6, 7 and references therein). This complicated problem requires a sophisticated approach based on three-dimensional modeling of the CO ignition and propagation of the thermonuclear flame that is fraught with specific unsteadinesses such as convective, Rayleigh-Taylor, Landau-Darries instabilities.

Such an investigation is of fundamental importance for the accurate calibration of SN Ia as the cosmological standard candles (one needs to predict the SN Ia peak luminosity at least with a 10% precision!). Also for detailed comparison with observations and for stellar nucleosynthesis, a precise determination of different isotopic yields (apart from dominating ^{56}Ni) is of vital importance.

1.2. Core-collapse supernovae

Type II SNe light curves are powered first by the shock heating, then by recombination of hydrogen, and finally (at their *tail phase*) by the $^{56}\text{Co} \rightarrow ^{56}\text{Fe}$ decay of $\approx (0.02 - 0.2) M_{\odot}$ of ^{56}Co (initially ^{56}Ni). The total energy of the electromagnetic emission is of $\approx 10^{49}$ erg.

The explosion energy of the core-collapse SNe is typically of $(0.5 - 2) \times 10^{51}$ erg. It comes from the shock wave that is launched somewhere at the boundary between the “iron” core of a mass $M_{\text{Fe}} = (1.2 - 2) M_{\odot}$, collapsing into a neutron star (NS), and the outer envelope to be thrown out. The mean velocity of the expansion is of 3,000 – 5,000 km/s depending on the mass of the envelope expelled.

The mechanism of the core-collapse SNe is not yet understood in every detail. The most distinctive feature of these SNe is an enormous energy of $(3 - 5) \times 10^{53}$ erg = (10 – 15)% $M_{\text{Fe}}c^2$ radiated in form of neutrinos and antineutrinos of all the flavors (e, μ, τ). One would think that it should not be a problem to extract less than 1% from the energy of a powerful neutrino flux to ensure the expulsion of the SNe envelope. However, an

extensive hydrodynamical modeling during the last thirty years has demonstrated that in case of spherical symmetry it is very hard (if not impossible) to simulate the explosion. Basing on this research, an empirical theorem can be formulated telling that spherically-symmetrical models do not result in expulsion of an envelope; the SN outburst does not occur: the envelope falls back on the collapsed core. Hence, one has to go to two- and, perhaps, three-dimensional models to convert the stalled accreting shock into an outgoing blast wave (for the last review see Ref. 8 and references therein). One has, nevertheless, to keep in mind that yet undiscovered elementary particles may be involved in the core-collapse SNe (e.g., axion-like particles⁹).

There are three reasons of spherical symmetry breakdown which currently are under a close investigation:

- *Large-scale neutrino-driven convection.*
The accreting shock can obtain an additional energy necessary for successful explosion from fast (possibly jet-like) subsonic streams of neutrino-heated matter circulating under and over the neutrinosphere.^{10,11,12,13}
- *Interaction between rotation and magnetic field.*
Hydrodynamical heterogeneity of the collapse (central dense layers of stellar core contract increasingly faster than outer ones) results in a strong differential rotation that leads to an amplification of toroidal magnetic field. Under favorable conditions, an excessive magneto-hydrodynamical pressure could facilitate the expulsion of the supernova envelope.^{14,15}
- *Rotational fragmentation followed by a NS explosion.*
Massive fast-rotating collapsed core undergoes rotational fragmentation resulting in formation of a close neutron-star binary that evolves being driven by the emission of gravitational waves and mass-exchange and terminates with a low-mass ($M \approx 0.1 M_{\odot}$) neutron-star explosion.^{16,17}

Figure 1 shows a general view of electromagnetic and neutrino luminosity of SNe. The SNIa bolometric light curve is given by a dashed line that includes all electromagnetic spectrum (uvoir + $X + \gamma$: ultraviolet, optical, infrared, X -rays, and gamma radiation). In ~ 40 days after explosion, the light curve strictly follows the ^{56}Co decay half-life of 77.1 days (111.3 days for exponential decay time). There is shown also the typical SNIIP light curve with a ~ 100 -day period of nearly constant luminosity (plateau) stabilized by a cooling-and-recombination wave.^{18,19} If there were no ^{56}Co in the supernova envelopes the light curves would be of a shorter duration (dotted curves). In the case of SN 1987A in the Large Magellanic Cloud, about $0.075 M_{\odot}$ of ^{56}Ni was synthesized.

Figure 2 shows the SN 1987A light curve on a large scale as observed by two group of astronomers in Chili²⁰ (black dots) and South Africa²¹ (open squares). A 20% discrepancy between these two sets of observations is a systematic uncertainty connected with reconstruction of the bolometric luminosity from luminosities observed in different spectral bands. The coincidence of the SN 1987A bolometric light curve with the Co-decay law at $t > 140$ days gave the first direct proof that supernova ejecta are actually enriched with theoretically predicted ^{56}Co . In a month, this finding was confirmed by the detection of

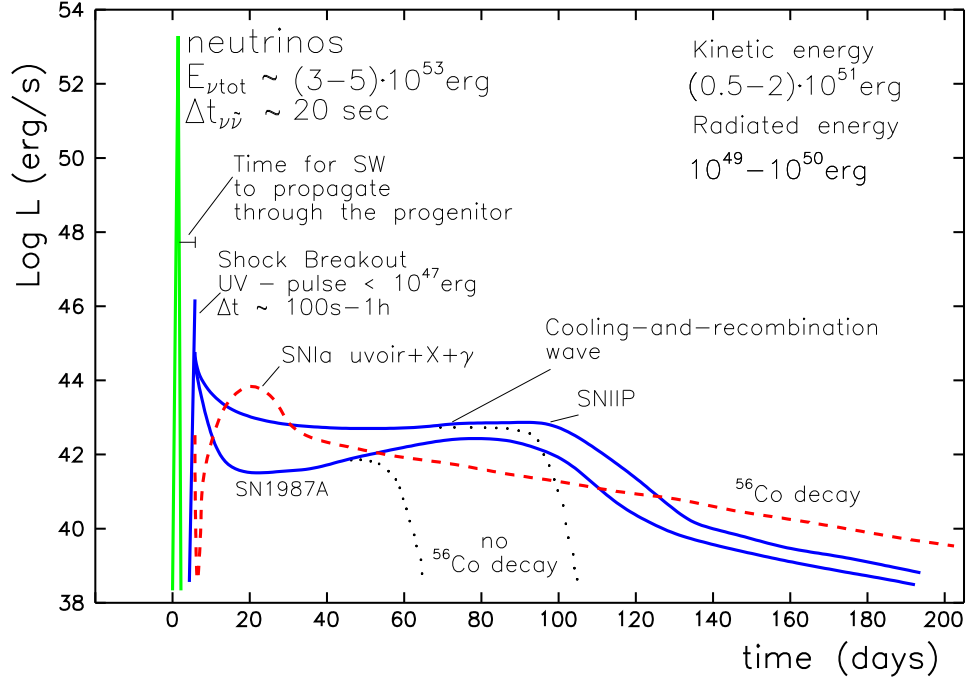


Fig. 1. A schematic illustration of the light curves and other supernova properties.

X-rays by space-based detectors *Kvant*²² and *Ginga*²³ and somewhat later by direct measurement of gamma-lines from Co-decay.²⁴ Detailed report on the SN 1987A event can be found in special reviews.^{25,26,27} For recent thorough study of the SN 1987A light curve on the basis of radiation hydrodynamics with nonthermal ionization from the ⁵⁶Ni and ⁵⁶Co decays included see Ref. 28.

2. Shock Wave Breakout

The onset of supernova outburst occurs at the very time when the outgoing shock wave (SW) reaches the stellar surface. Such a breakout results in a short pulse of ultraviolet and soft X-ray radiation of total energy up to 10^{47} erg and with characteristic duration of 100s–1h depending on the presupernova radius (Fig. 1). The “tail” of this pulse was actually observed in the case of SN 1987A (Fig. 2). The shock wave propagates through stellar interior outward in the direction of strongly decreasing density. Consequently, the shock energy turns out to be accumulated in a progressively decreasing amount of matter. As a result, the SW considerably accelerates as illustrated in Fig. 3. Such a cumulative regime is described by well-known similarity solution of hydrodynamic equations that exists since the density ρ typically is a power function of the distance x to stellar surface $\rho \sim x^n$ ($n \approx 3$). Formally, the velocity tends to infinity at stellar surface (short-dashed curve for $t = 0$). In reality, the SW cumulation is limited by a finite width of the SW front which optical thickness $\Delta\tau$

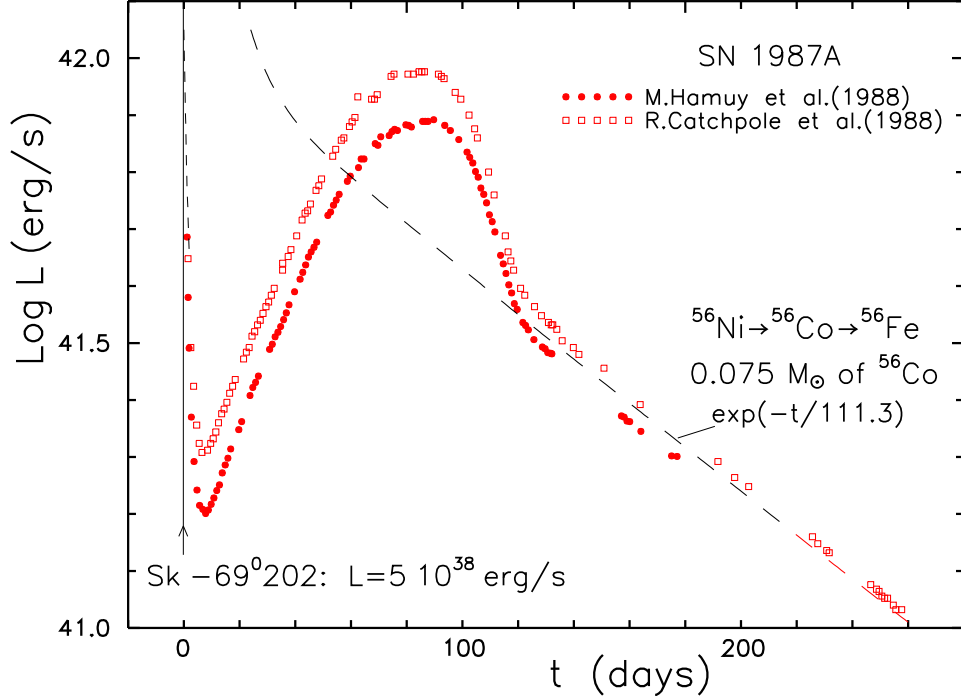


Fig. 2. The bolometric light curve of SN 1987A exploded on February 23, 1987. Time is measured from the moment of the shock wave breakout. At $t \approx 90$ days, the SN 1987A luminosity attains a maximum of $\approx 10^{42}$ erg/s that by a factor of 2,000 exceeds the luminosity of the progenitor, blue supergiant Sk-69°202. The shock wave breakout “tail” is shown by a nearly vertical dashed line at $t \approx 0$. (Adapted from Ref. 19).

for the radiation dominated SW can be estimated from a simple relation: $\Delta\tau \approx c/D$, with D and c being the SW velocity and the speed of light, respectively. The distance x_{cut} at which one has to cut the similarity solution off corresponds to the SW position when its optical depth becomes just equal to $\Delta\tau$ (see Ref. 29). With x_{cut} known one can estimate the maximum velocity at the SW front emerging from under the stellar surface. During further expansion (curves for $t > 0$ in Fig. 3), matter undergoes additional acceleration in a rarefaction wave that converts almost all thermal energy into kinetic energy of radial expansion increasing the latter by a factor of ≈ 2.6 (Ref. 30).

For SN 1987A, x_{cut} is estimated to be $\approx 0.02R_0$ ($R_0 \approx 47R_\odot$ is the presupernova radius). The resulting final maximum velocity u_{max} relating to kinetic energy per nucleon $\varepsilon_{\text{max}} = \frac{1}{2}m_u u_{\text{max}}^2$ (m_u is the atomic mass unit) and the mass $\Delta M_{u_{\text{max}}}$ accelerated to the maxim velocity u_{max} turn out to be:¹⁹

$$u_{\text{max}} \approx 40,000 \text{ km/s}, \quad \varepsilon_{\text{max}} \approx 8.3 \text{ MeV/nucleon}, \quad \Delta M_{u_{\text{max}}} \approx 2 \times 10^{-6} M_\odot.$$

The SW breakout was expected³¹ to be an efficient mechanism for acceleration of cosmic rays. For SN 1987A this mechanism, however, does not look effective enough. Since the maximum kinetic energy changes with R_0 as $R_0^{-0.65}$, one can think of the SN explo-

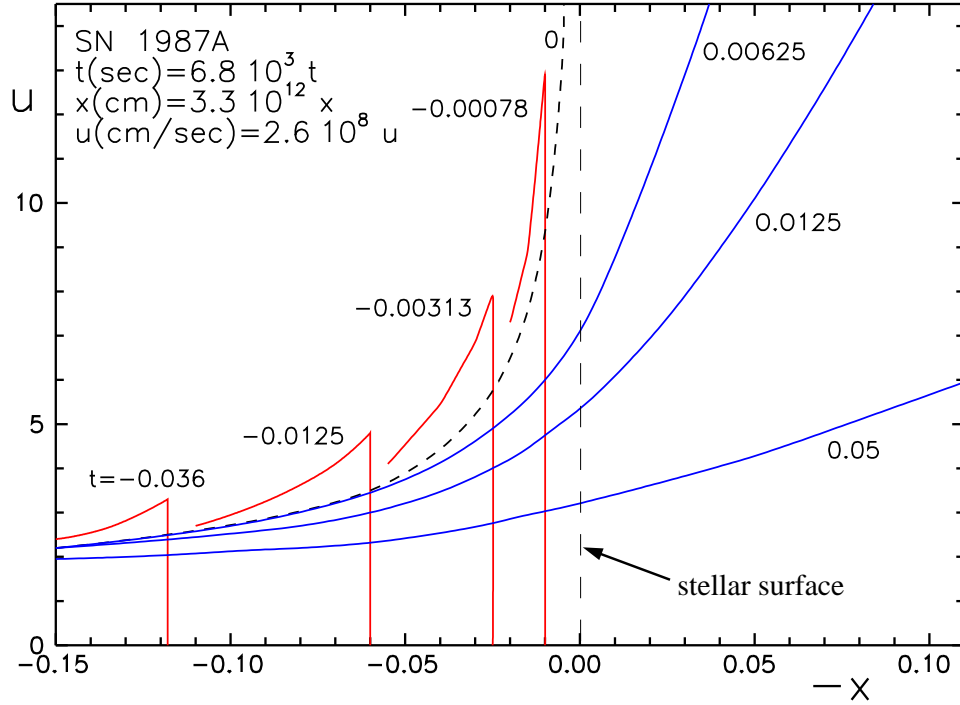


Fig. 3. Velocity u versus distance x from stellar surface at different points of time t during the shock wave breakout. It is assumed that $t = 0$ when the shock reaches the surface (short-dashed curve). The equations one must use to convert u , x , and t to dimensional units (cm, sec) are shown for the case of SN 1987A. (Adapted from Ref. 19).

sions associated with presupernovae of smaller radii. The SN Ib and SN Ic can have as small R_0 as a few R_\odot and ε_{\max} may reach about 100 MeV/nucleon for these SNe. The explosion of a white dwarf of typical radius (5,000 – 10,000) km would be just the right event to accelerate a good portion of matter to relativistic energies ($\varepsilon_{\max} \gtrsim 1$ GeV/nucleon). However, the regime of the SW cumulation does not occur in the case of SNe Ia that come from white dwarf progenitors. The thermonuclear burning begins there in a deflagration regime causing the star to expand subsonically. Even though the SW does appear this happens at the very end of the explosion under the conditions unfavorable for the SW cumulation.

Although, to all appearance, the direct hydrodynamical acceleration of CR in supernovae turns out to be inefficient the SW breakout could provide fast moving particles for further acceleration by other mechanisms (e.g., by circum-stellar and interstellar shock waves).

3. Shock Waves in Circum-Stellar Medium

In a few days after explosion, the SN envelope turns into a state of supersonic inertial expansion with the velocity depending on radius by the simplest way: $u = r/t$ where the

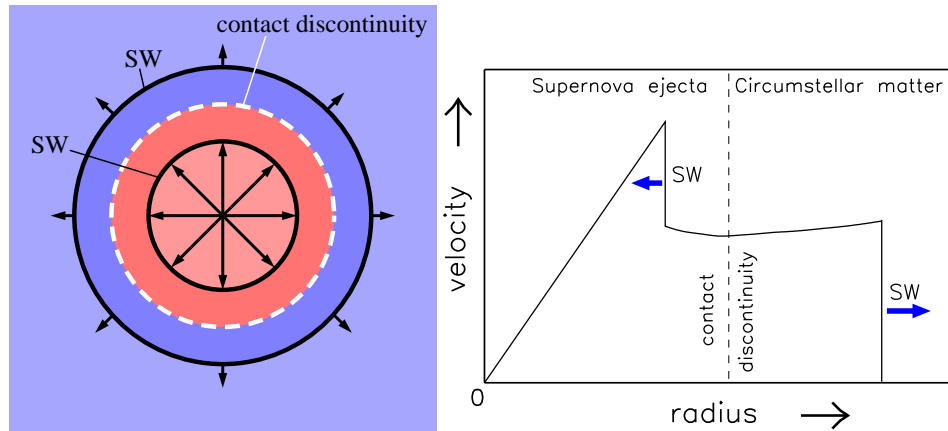


Fig. 4. A schematic illustration of the interaction between the SN ejecta and ambient medium: general hydrodynamic layout (left panel) and velocity versus radius in arbitrary units (right panel).

time t is measured from the beginning of the explosion. Simultaneously the outer edge of the SN envelope begins to collide with the circum-stellar matter. The interaction region is confined by two shock waves shown in Fig. 4 (left panel) by black circles. The SN ejecta are decelerated, heated, and compressed by the internal (reverse) SW. The outer (forward) SW accelerates, heats and compresses the ambient medium. Thus, *relative to matter* the reverse and forward shock waves propagate in an inward and outward direction, respectively. This is shown by arrows in Fig. 4 (right panel). The interface separating the shocked ejecta from shocked interstellar matter called *contact discontinuity* is shown by a white dashed circle in Fig. 4 (left panel).

The hydrodynamic theory of the SN ejecta – ambient medium interaction has been elaborated with the help of numerical and semi-analytical methods (see Ref. 32 and references therein). The initial stage of this *ejecta-dominated* process is controlled by a similarity solution^{33,34} that being combined with observations allows to describe detailed structure of young supernova remnants (SNRs). A few hundred years old remnants of galactic supernovae such as Cas A, Kepler, Tycho are still in the ejecta-dominated stage. Observations of their X-ray and radio synchrotron emission can give much information about the SN progenitor, supernova nucleosynthesis,³⁵ ambient medium, and mechanisms of the cosmic-ray acceleration.

4. Core-Collapse Neutrinos

The collapse of stellar iron-cores into a neutron star (NS) is followed by a high-power pulse of neutrino emission. Figure 5 shows the cumulative (bolometric) neutrino light curve that includes all the neutrino and antineutrino flavors. This light curve was calculated for a spherically symmetrical collapse of a $2 M_{\odot}$ stellar core.³⁶ According to detailed modeling during the past few decades of the neutrino transport in collapsing stellar cores, this light curve consists of two parts.

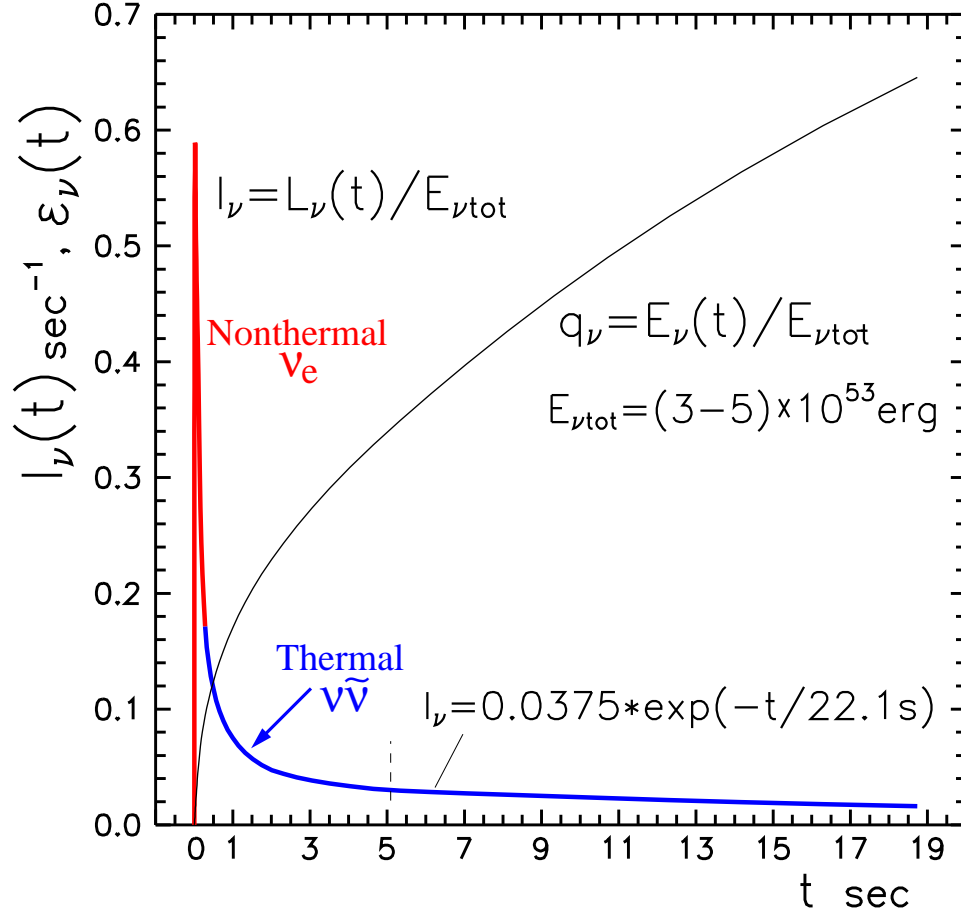


Fig. 5. The normalized bolometric neutrino light curve. The time t is measured from the beginning of the collapse. (Based on Ref. 36).

The first part ($t \lesssim 0.5$ s) relates to the nonthermal neutrino emission that is dominated by the electron neutrinos ν_e produced by the non-equilibrium neutronization. For $t \lesssim 0.5$ s, the core is still transparent to ν_e emitted owing to electron captures by nuclei and free protons. The mean individual ν_e energy ε_{ν_e} turns out to be 15 – 20 MeV. The nonthermal neutrinos carry away only a small fraction ($q_\nu \lesssim 10\%$, Fig. 5) of the total available energy $E_{\nu\text{tot}} = (3 - 5) \times 10^{53}$ erg.

About 90% of $E_{\nu\text{tot}}$ is emitted in the regime of thermal emission when the central region of the core becomes opaque to all the neutrino flavors. The neutrinos are decoupled from stellar matter at a surface called *neutrinosphere*. In general, the neutrinosphere radius is different for different neutrino flavors, at least one has to consider two neutrinospheres — one for the electron neutrinos and antineutrinos and another for μ - and τ -neutrinos and antineutrinos. Numerical modeling^{37,38} shows that to a first approximation one can assume

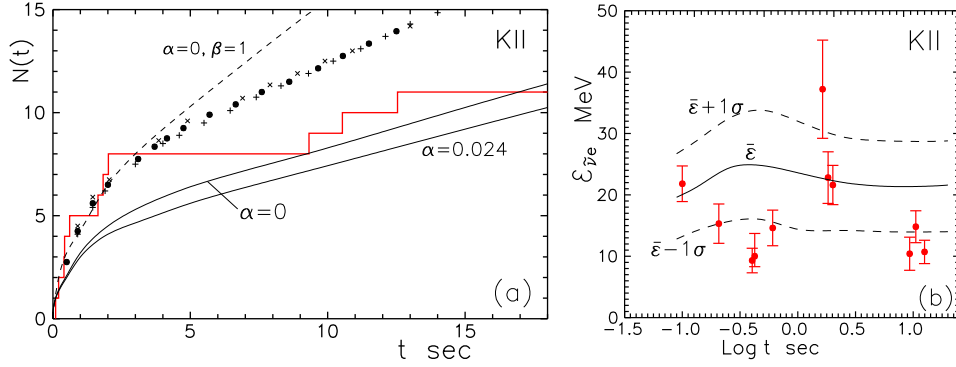


Fig. 6. A comparison of the neutrino signal predicted for SN 1987A with the response of the KamokaNDE II detector.⁴⁰ (a) The number of counts versus time in the detector (in total 11 events, step line). Different theoretical versions are also shown (see Ref. 25 for details). (b) The energy measured for every count in comparison with a theoretical prediction $\bar{\epsilon}$ bounded by $\pm 1\sigma$ uncertainty band. (From Ref. 25).

that $E_{\nu_{\text{tot}}}$ is equally distributed over the neutrino flavors:

$$E_{\nu\tilde{\nu}_e} \approx E_{\nu\tilde{\nu}_\mu} \approx E_{\nu\tilde{\nu}_\tau} \approx \frac{1}{3}E_{\nu_{\text{tot}}}.$$

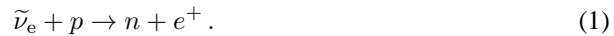
The neutrino spectra are reproduced by the Fermi–Dirac distributions slightly depressed³⁹ at high energies $\epsilon \gg kT_{\nu_{\text{ph}}}$ ($T_{\nu_{\text{ph}}}$ is the effective temperature of the neutrinosphere). The mean individual neutrino energies and related $T_{\nu_{\text{ph}}}$ are

$$\langle \epsilon \rangle_{\nu\tilde{\nu}_e} \approx (10 - 12) \text{ MeV}, \quad \langle \epsilon \rangle_{\nu\tilde{\nu}_\mu} \approx \langle \epsilon \rangle_{\nu\tilde{\nu}_\tau} \approx 25 \text{ MeV},$$

$$T_{\nu\tilde{\nu}_e\text{ph}} \approx 4 \text{ MeV}, \quad T_{\nu\tilde{\nu}_\mu\text{ph}} \approx T_{\nu\tilde{\nu}_\tau\text{ph}} \approx 8 \text{ MeV}.$$

The characteristic time of the neutrino pulse turns out to be of the order of 10–20 s.

These theoretically predicted properties seem to be in a fair agreement with the neutrino signal detected from SN 1987A by the KamiokaNDE II (K II)⁴⁰ and Irvine-Michigan-Brookhaven (IMB)⁴¹ neutrino detectors as it is shown in Fig. 6 for K II. The agreement occurs under the assumption that all the events in these water Cherenkov detectors were produced by the electron antineutrinos through the reaction



In contrast to the neutrino-electron scattering, the relativistic positrons from this reaction move virtually isotropically in different directions. So the direction of their Cherenkov radiation should not depend on where $\tilde{\nu}_e$ has come from. However, one can observe that the events with energies $\epsilon_{\tilde{\nu}_e} \gtrsim 20 \text{ MeV}$ (four events in Fig. 6 and all eight events recorded by the IMB detector) demonstrate a statistically significant correlation with the direction to the Large Magellanic Cloud. Since the neutrino-electron scattering cross-section is considerably lower than that of the reaction (1) it is impossible to explain this observation by addressing to the $\nu_{\mu\tau}$ -electron scattering — the required total energy of the neutrino pulse would exceed by an order of magnitude the energy available from the collapse of

stellar cores. The significance of this problem (remaining unresolved up to now!) was first recognized and analyzed in Refs. 42, 43.

Another difficulty in the theoretical interpretation of the SN 1987A neutrino signal is the fact that there occurred *two* neutrino pulses. The first pulse, detected by the Liquid Scintillation Detector (LSD) under Mont Blanc,^{44,45} came 4.7 hours earlier than the second one recorded by the K II and IMB detectors. Since 4.7 h is a very long time in comparison with the duration of both the neutrino pulses (~ 10 s), one has to think of a two-stage collapse (see discussion in Ref. 25). In the next section, we describe a scenario that has been recently proposed⁴⁶ to incorporate both the neutrino pulses in a self-consistent two-stage hydrodynamical model of the gravitational collapse.

5. Rotational Fragmentation—Neutron Star Explosion Scenario

The key point for this scenario is the presence of rotation in the stellar core that is about to collapse. The mechanism of the SN explosion proposed in Ref. 16 is based on the rotational instability and develops through the following stages.

First, the rotational energy of the collapsing core E_{rot} reaches the limit of stability with respect to fragmentation:⁴⁷ $E_{\text{rot}}/|E_{\text{g}}| > 0.27$ (E_{g} is the core gravitational energy).

Then the core of mass M_0 fragments into a close binary system of proto-neutron stars of different masses M_1 and M_2 ($M_1 + M_2 = M_0$; we assume $M_2 < M_1$ hereafter).

These binary components begin to approach each other due to the loss of total angular momentum and kinetic energy of orbital motion through the radiation of gravitational waves (GW):⁴⁸

$$L_{\text{GW}}(t) = \frac{32 G^4 (M_1 + M_2) M_1^2 M_2^2}{5 c^5 a^5(t)} \approx 10^{52-55} \text{ erg/s}, \quad (2)$$

where L_{GW} is the GW luminosity, G is the gravitational constant, and c is the speed of light. The mutual approach of the components lasts until the orbital radius $a(t)$ reaches a critical value $a = a_{\text{cr}}$ for which the *less massive* component fills its Roche lobe. Contrary to normal stars, the degenerate configurations like NSs and white dwarfs have a remarkable property: the smaller their mass, the larger their radius ($R \sim M^{-1/3}$).

As soon as a becomes less than a_{cr} , there begins a rapid mass transfer from the component M_2 to the component M_1 . The mass M_2 is rapidly decreasing down to the minimum possible mass of a NS $M_{\text{NSm}} \approx 0.1 M_{\odot}$. When M_2 becomes a little bit less than M_{NSm} , the process of the hydrodynamic destruction of a low-mass component begins. Such a dynamical instability is controlled by the rate of beta-processes, and initially is developing rather slowly. It terminates, however, with a short (~ 0.05 s) phase of a violent transformation of the internal energy into kinetic energy and work against gravity. The resulting energy release is expected to be as large as $\sim 10^{51}$ erg (~ 4.8 MeV per nucleon). However, the sophisticated calculations are still to be done to estimate how much of the energy is taken away by neutrinos. The hydrodynamics of the low-mass NS explosion was studied in a number of papers (see Refs. 49, 50 and references therein).

The low-mass NS explosion model has no problems with the explanation of the explosion asymmetry (like that observed for SN 1987A) and the origin of the high-velocity

pulsars. The debris of exploded low-mass NS ($0.1 M_{\odot}$) and the collapsed NS ($\sim 1.5 M_{\odot}$) retain their orbital velocities of (7500–15000) and (500–1000) km/s, respectively, and move in opposite directions.⁵¹ There is no problem in this scenario also with dissociating of the heavy elements in the infalling envelope.

Thus in this scenario, the supernova outburst is triggered by the explosion of a low-mass NS. The most impressive feature of the scenario is its ability to explain the two neutrino signals from SN 1987A in the framework of a single self-consistent model.

Table 1. Responses of the neutrino detectors to the $\nu_e A$ interaction for the Mont Blanc (LSD), KamiokaNDE II (KII), and Baksan (BUST) events. (Adapted from Ref. 46).

Detector	Energy threshold MeV	Predicted number N of interactions	Predicted counts $N\eta$	Actually detected
LSD	5 – 7	5.7	3.2	5 (Refs. 44, 45)
KII	7 – 14	3.1	2.7	3 (Ref. 52)
BUST	10	5.2	~ 1	1 (Ref. 53)

The first recorded by LSD neutrino pulse comes from the first stage of the collapse when there occurs the rotational fragmentation of stellar core into two proto-neutron stars. This is essentially a three-dimensional process. A strongly flattened by rotation structure of the core favors the emission of highly non-thermal *electron* neutrinos with the individual energies of (30–40) MeV that appear owing to capture of strongly degenerate electrons by atomic nuclei and free protons ($p + e^- \rightarrow n + \nu_e$). When such energetic ν_e 's reach the LSD detector they interact with 200 tons of the iron safety and radioactivity shield around 90 tons of scintillator (white spirit). The cross-section of the reaction $\nu_e + {}^{56}\text{Fe} \rightarrow {}^{56}\text{Co}^* + e^-$ proved to be of the order of $4 \times 10^{-40} \text{ cm}^2$ – just appropriate value to interpret with a statistically good accuracy the observed five LSD events as a response of scintillator to gamma rays from deexcitation of ${}^{56}\text{Co}^*$ and to the electrons. Similar effect (however with a lower cross-section) occurs due to ν_e interaction with such heavy constituents of the scintillator itself as ${}^{12}\text{C}$ and ${}^{16}\text{O}$. Table 1 presents the responses of different detectors to the $\nu_e - A$ interaction ($A = {}^{56}\text{Fe}$ for LSD and BUST, and ${}^{16}\text{O}$ for K II). The KII and BUST detectors could not confidently detect the first neutrino pulse owing to their higher than for LSD thresholds and backgrounds (for further details see Ref. 46).

The second neutrino pulse occurs approximately at the moment of the low-mass NS explosion when more massive NS component ($M_1 = M_0 - M_{\text{NSm}}$), having been already deprived of a good portion of its angular momentum, resumes the collapse to produce a powerful burst of more or less thermal neutrinos described in previous section.

The time interval of 4.7 h separating the two neutrino pulses is controlled by the GW radiation and can be easily explained by the evolution of the NS binary system that is described by a semi-analytical approach.^{17,48,55}

In the future, the proposed scenario can be verified with the aid of the GW detectors such as VIRGO and LIGO, at least within the Milky Way distances of $D \approx 10 \text{ kpc}$. The

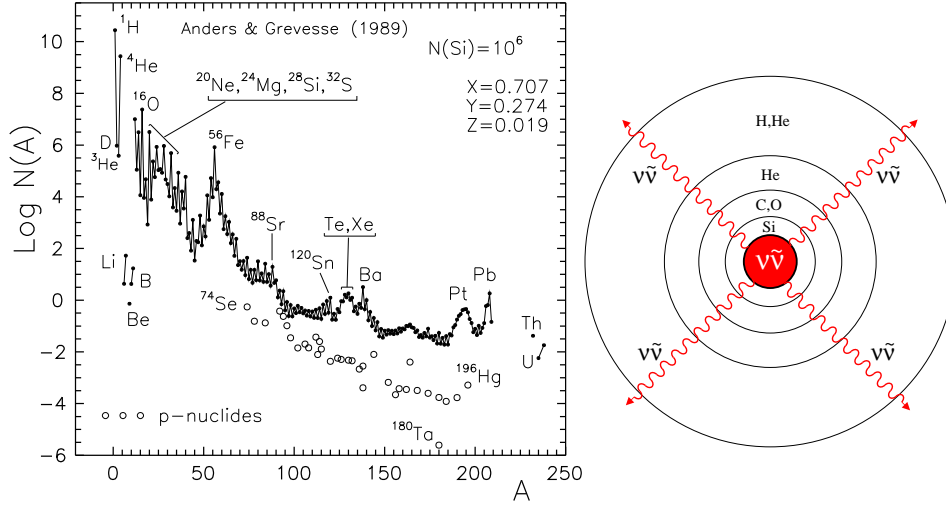


Fig. 7. The cosmic abundances of chemical elements⁵⁴ versus the mass number A . The p-nuclides are shown explicitly (left panel). The onion-like presupernova structure (right panel).

amplitude of metric perturbation in question is estimated⁴⁸ to be

$$h = \frac{8 G^2 M_1 M_2}{\sqrt{5} c^4 a D} \approx (1 - 0.2) \times 10^{-18}, \quad D = (10 - 50) \text{ kpc}. \quad (3)$$

According to a conservative estimate, the gravitational waves carry away in total 10^{50-52} erg within a frequency range (100–3000) Hz.

6. Neutrino Nucleosynthesis

The neutrinos from collapsed stellar cores can produce a number of nuclear transmutations in the onion-like structured envelope (Fig. 7, right panel) to be thrown off by the blast wave.^{56,57,58,59} With the aid of neutrinos, it is possible to overcome difficulties in interpreting the cosmic abundances of such nuclear species as (i) p-nuclides that cannot be produced in the neutron-capture processes, (ii) a number of rare nuclides (^{15}N , ^{19}F , ^{26}Al , ^{50}V and some others), and (iii) the light elements (Li, Be, B). The magnitude $\delta n(A, Z)$ of the neutrino-induced transformation in the reaction $\nu + (A, Z) \rightarrow \dots$ can be estimated from a simple equation

$$\frac{\delta n(A, Z)}{n(A, Z)} = N_\nu \frac{\langle \sigma_{n\nu} \rangle}{4\pi r^2} = \frac{E_\nu}{\langle \varepsilon_\nu \rangle} \frac{\langle \sigma_{n\nu} \rangle}{4\pi r^2} \approx (0.01 - 0.1), \quad (4)$$

where N_ν , $\langle \sigma_{n\nu} \rangle$, and r are the total number of emitted neutrinos responsible for the transformation, their energy-averaged cross-section, and the distance of the neutrino-irradiated matter, respectively. Each of three $\nu\bar{\nu}$ flavors can be involved in the transformation (4). The numerical quantity is estimated for typical values $N_\nu = 3 \times 10^{57}$, $r = 10^9$ cm, and $\langle \sigma_{n\nu} \rangle = (3 - 30) \times 10^{-41} \text{ cm}^2$.

The creation of the light elements is a field of overlap between the contributions from cosmic rays (CR), big bang nucleosynthesis (BBN) and neutrino nucleosynthesis (NN). The neutrino flux proves to be especially efficient in production of ${}^7\text{Li}$ (in helium shell) and ${}^{11}\text{B}$, ${}^9\text{Be}$ (in CO-shell). At the same time, it is not so effective in producing of ${}^6\text{Li}$ and ${}^{10}\text{B}$. Thus, the large cosmic ratios⁵⁴ ${}^7\text{Li}/{}^6\text{Li}= 12.3$ and ${}^{11}\text{B}/{}^{10}\text{B}= 4.02$ can be easily understood in the framework of neutrino nucleosynthesis. And there is no need to invoke a hypothetical low-energy ($E \lesssim 100$ MeV) cosmic rays to explain these ratios. Presumably, cosmic abundances of the light element isotopes can be considered as coming from combinations of contributions from BBN, CR, and NN: ${}^6\text{Li}$ (CR), ${}^7\text{Li}$ (BBN+CR+NN), ${}^9\text{Be}$ (CR+NN), ${}^{10}\text{B}$ (CR), and ${}^{11}\text{B}$ (CR+NN). One has also to keep in mind other possible stellar sources of the light elements, e.g. such as novae and red giant (AGB) stars.

7. Gamma-Ray Burst – Supernova Connection

Cosmic source of the gamma-ray bursts (GRBs) discovered 30 years ago^{60,61} long remained actually unknown. The breakthrough in understanding of the GRBs happened in late 90ths. There was discovered⁶² that at least some GRBs were followed by afterglows. Then the afterglow was found to be connected to supernovae.^{63,64} This findings allowed to couple GRBs with host galaxies of known redshifts and thereby directly to confirm previously assumed cosmological distances (of hundreds Megaparsecs) to the GRBs. The most convincing proof of the GRBs–SNe connection came from Chandra’s 21-hour (!) X-ray exposure of the afterglow associated with the GRB detected on 13 August 2002 that allowed to identify narrow lines due to silicon and sulfur ions inherent to the SN ejecta.⁶⁵

The GRB mechanism is not yet well understood. However, the gamma-rays are thought to be beamed into a narrow cone along a jet of high energy relativistic particles expelled from a supernova core that has just collapsed into either a NS or a black hole (see Refs. 66, 67, 68, 69 and references therein). Such jets seem to occur 10–60 d after the beginning of the collapse. They interact with the expanding supernova envelope and produce the X-ray and optical afterglows.^{70,71} The core-collapse SNe Ib and Ic are expected to be the best sites for creating the GRBs. These SNe are deprived of dense hydrogen-rich envelopes that would prevent gamma-rays to escape from the star.

The jet-like streams of relativistic particles can be a good starting point for writing a new chapter in the theory of origin of cosmic rays.⁷² The GRBs–SNe connection opens a new intriguing approach to understanding the mechanism of the core-collapse SNe.

Acknowledgments

D.K.N. has a pleasure to thank the Institute for Nuclear Research of Russian Academy of Sciences and Laboratori Nazionali del Gran Sasso of Istituto Nazionale di Fisica Nucleare (Italy) and their staffs for warm hospitality during his staying in Italy. The work was supported by the Russian Foundation for Basic Research (project no. 04-02-16793-a).

References

1. A. M. Khokhlov, *Astron. Astrophys.* **246**, 383 (1991).
2. S. E. Woosley and T. A. Weaver, in *Supernovae, Les Houches, Session LIV*, ed. S. A. Bludman, R. Mochkovitch and J. Zinn-Justin, (Elsevier Sci., Amsterdam, 1994), p. 63.
3. L. N. Ivanova, V. S. Imshennik and V. M. Chechetkin, *Astrophys. Space Sci.* **31**, 497 (1974).
4. N. G. Dunina-Barkovskaya, V. S. Imshennik and S. I. Blinnikov, *Astron. Lett.* **27**, 353 (2001).
5. S. E. Woosley, S. Wunsch and M. Kuhlen, *Astrophys. J.* **607**, 921 (2004).
6. F. K. Röpkke and W. Hillebrandt, astro-ph/0409286, v.1 (13 Sep. 2004).
7. V. N. Gamezo, A. M. Khokhlov and E. S. Oran, astro-ph/0409598, v.1 (24 Sep. 2004).
8. A. Burrows, R. Walder, C. D. Ott and E. Livne, astro-ph/0409035, v.1 (1 Sep. 2004).
9. Z. Berezhiani *et al.*, *Astrophys. J.* **586**, 1250 (2003).
10. R. I. Epstein, *Mon. Not. Roy. Astron. Soc.* **188**, 305 (1979).
11. M. Livio, J. R. Buchler, and S. A. Colgate, *Astrophys. J.* **238**, L139 (1980).
12. J. M. Lattimer and T. J. Mazurek, *Astrophys. J.* **246**, 955 (1981).
13. V. S. Imshennik, *Yad. Fiz.* **65**, 2138 (2002).
14. G. S. Bisnovatyi-Kogan, *Astron. Zh. Akad. Nauk SSSR* **47**, 813 (1970).
15. S. G. Moiseenko, G. S. Bisnovatyi-Kogan and N. V. Ardeljan, astro-ph/0410330, v.1 (13 Oct. 2004).
16. V. S. Imshennik, *Sov. Astron. Lett.* **18**, 194 (1992).
17. V. S. Imshennik and D. V. Popov, *Astron. Lett.* **20**, 529 (1994).
18. E. K. Grasberg, V. S. Imshennik and D. K. Nadyozhin, *Astrophys. Space Sci.* **10**, 3 (1971).
19. D. K. Nadyozhin, in *Supernovae, Les Houches, Session LIV*, eds. S. A. Bludman, R. Mochkovitch and J. Zinn-Justin, (Elsevier Sci., Amsterdam, 1994), p. 571.
20. M. Hamuy, N. B. Suntzeff, R. Gonzalez and G. Martin, *Astron. J.* **95**, 63 (1988).
21. R. M. Catchpole *et al.*, *Mon. Not. Roy. Astron. Soc.* **231**, 75P (1988).
22. R. A. Sunyaev *et al.*, *Nature* **330**, 227 (1987).
23. T. Datani *et al.*, *Nature* **330**, 230 (1987).
24. S. M. Matz *et al.*, *Nature* **331**, 416 (1988).
25. V. S. Imshennik and D. K. Nadyozhin, *Sov. Sci. Rev. Sect. E: Astrophys. Space. Phys. Rev.* **8**, part 1, 156 (1989).
26. W. D. Arnett *et al.*, *Ann. Rev. Astron. Astrophys.* **27**, 629 (1989).
27. D. K. Nadyozhin, in *Proceedings of the International School on Particles and Cosmology*, eds. V. A. Matveev *et al.* (World Scientific Publishing Co., Singapore, 1992), p. 153.
28. V. P. Utrobin, *Astron. Lett.* **30**, 334 (2004).
29. V. S. Imshennik and D. K. Nadyozhin, *Sov. Astron. Lett.* **14**, 449 (1988).
30. I. Yu. Litvinova and D. K. Nadyozhin, *Sov. Astron. Lett.* **16**, 29 (1990).
31. S. A. Colgate and M. H. Johnson, *Phys. Rev. Lett.* **5**, 235 (1960).
32. J. K. Truelove and C. F. McKee, *Astrophys. J. Supp.* **120**, 299 (1999).
33. R. A. Chevalier, *Astrophys. J.* **258**, 790 (1982).
34. D. K. Nadyozhin, *Astrophys. Space Sci.* **112**, 225 (1985).
35. A. Decourchelle *et al.*, *Astron. Astrophys.* **365**, L218 (2001).
36. D. K. Nadyozhin, *Astrophys. Space Sci.* **53**, 131 (1978).
37. S. W. Bruenn, *Astrophys. J. Supp.* **58**, 771 (1985).
38. S. W. Bruenn, *Phys. Rev. Lett.* **59**, 938 (1987).
39. D. K. Nadyozhin and I. V. Otroshchenko, *Sov. Astron.* **24**, 47 (1980).
40. K. Hirata *et al.*, *Phys. Rev. Lett.* **58**, 1490 (1987).
41. R. M. Bionta *et al.*, *Phys. Rev. Lett.* **58**, 1494 (1987).
42. O. G. Ryazhskaya and V. G. Ryasnyi, *JETP Lett.* **47**, 283 (1988).
43. V. L. Dadykin, G. T. Zatsepin and O. G. Ryazhskaya, *Sov. Phys. Usp.* **32**, 459 (1989).
44. V. L. Dadykin *et al.*, *JETP Lett.* **45**, 593 (1987).

45. M. Aglietta *et al.*, *Europhys. Lett.* **3**, 1321 (1987).
46. V. S. Imshennik and O. G. Ryazhskaya, *Astron. Lett.* **30**, 14 (2004).
47. J. L. Tassoul, *Theory of Rotating Stars* (Princeton Univ. Press, 1978).
48. V. S. Imshennik and D. V. Popov, *Astron. Lett.* **24**, 206 (1998).
49. S. I. Blinnikov *et al.*, *Sov. Astron.* **34**, 595 (1990).
50. M. Colpi, S. L. Shapiro and S. A. Teukolsky, *Astrophys. J.* **414**, 717 (1993).
51. A. G. Aksenov *et al.*, *Astron. Lett.* **23**, 677 (1997).
52. A. De Rujula, *Phys. Lett.* **B193**, 514 (1987).
53. E. N. Alexeyev *et al.*, *JETP Lett.* **45**, 589 (1987).
54. E. Anders and N. Grevesse, *Geochim. Cosmochim. Acta* **53**, 197 (1989).
55. V. S. Imshennik and D. V. Popov, *Astron. Lett.* **28**, 465 (2002).
56. G. V. Domogatsky and D. K. Nadyozhin, *Sov. Astron.* **22**, 297 (1978).
57. G. V. Domogatsky, R. A. Eramzhyan and D. K. Nadyozhin, *Astrophys. Space Sci.* **58**, 273 (1978).
58. S. E. Woosley *et al.*, *Astrophys. J.* **356**, 272 (1990).
59. A. Heger *et al.*, *Nucl. Phys.* **A718**, 159 (2003).
60. R. Klebesadel, I. Strong and R. Olson, *Astrophys. J.* **182**, L85 (1973).
61. E. P. Mazets, S. V. Golenetskii and V. N. Ilinskii, *JETP Lett.* **19**, 77 (1974).
62. E. Costa *et al.*, *Nature* **387**, 783 (1997).
63. S. R. Kulkarni *et al.*, *Nature* **395**, 663 (1998).
64. T. J. Galama *et al.*, *Nature* **395**, 670 (1998).
65. N. R. Butler *et al.*, *Astrophys. J.* **597**, 1010 (2003).
66. S. E. Woosley, *Astrophys. J.* **405**, 273 (1993).
67. S. Blinnikov, *Surveys High Energ. Phys.* **15**, 37, (2000).
68. K. Postnov, astro-ph/0410349, v.1 (14 Oct. 2004).
69. S. E. Woosley and A. Heger, *Astrophys. J.* in press (2004) [astro-ph/0309165].
70. C. D. Matzner, *Mon. Not. Roy. Astron. Soc.* **345**, 575 (2003).
71. D. I. Kosenko *et al.*, *Astron. Lett.* **29**, 206 (2003).
72. A. Dar, astro-ph/0408310, v.1 (17 Aug. 2004).